THE NEW SYNCHROTRON LIGHT SOURCES - POWERFUL TOOLS FOR RESEARCH AND PRODUCTION

Mark Pleško
Jožef Stefan Institute, Ljubljana, Slovenia

INVITED PAPER
23rd International Conference on Microelectronics, MIEL'95
31st Symposium on Devices and Materials, SD'95
September 27.-September 29., 1995, Terme Čatež, Slovenia

Key words: synchrotron radiation, synchrotron light sources, VLSI circuits, circuit production, VLSI devices, micro mechanic devices, device production, properties of synchrotron light, experimental methods, XAS, X-ray Absorption Spectroscopy, XANES, X-ray Absorption Near Edge Structure, EXAFS, Extented X-ray Absorption Fine Structure, XSW, X-ray standing waves, XRF X-Ray Fluorescence spectroscopy, EPS, electron photoemission spectroscopy, HREELS, High Resolution Electron Energy Loss Spectroscopy, measuring methods, ESCA, Electron Spectroscopy for Chemical Analysis, XRD, X-Ray Diffraction, WAYS, Wide Angle X-ray scattering, SAXS, Small Angle X-ray Scattering, LEED, Low Energy Electron Diffraction, LIGA, lithography, electroplating, moulding process

Abstract: In the last two years, new high-brilliance synchrotron light sources have been commissioned and taken into operation. Compact synchrotron sources dedicated to the production of VLSI and micro mechanic devices are being built, too. This article gives a basic list of the properties of synchrotron radiation, provides a brief overview of the main experimental methods and shows how synchrotron radiation can be used for production of micro devices. The new synchrotron light source ELETTRA, which has been built at Trieste, and the planned Slovenian beam line BOSS are presented in more detail.

Novi izvori sinhrotronske svetlobe. Močno orodje za raziskave in proizvodnjo

Ključne besede: sevanje sinhrotronsko, viri svetlobni sinhrotronski, VLSI vezja, proizvodnja vezij, VLSI naprave, naprave mikromehanske, proizvodnja naprav, lastnosti svetlobe sinhrotronske, metode eksperimentalne, XAS spektroskopija absorpcijska z Rentgen 'arki, XANES absorpcija struktur blizu roba z Rentgen žarki, EXAFS absorpcija Rentgen žarkov struktur finih razširjena, XSW valovi stojni Rentgen žarkov, XRF spektroskopija fluorescenčna z Rentgen žarki, EPS spektroskopija elektronska fotoemisijska, HREELS spektroskopija ločljivosti visoke z izgubo energije elektronov, metode merilne, ESCA spektroskopija elektronska za analizo kemično, XRD uklon Rentgen žarkov, WAXS stresanje Rentgen žarkov širokokotno, SAXS stresanje Rentgen žarkov ozkokotno, LEED difrakcija elektronov energije nizke, LIGA proces litografije, galvanizacije, odtisa tipografskega

Povzetek: Večje število novih izvorov sinhrotronske svetlobe z veliko svetilnostjo je bilo postavljeno in spuščeno v pogon v zadnjih dveh letih. Ravno tako so tudi mnogi kompaktni sinhrotronski izvori namenjeni proizvodnji VLSI vezij in mikromehanskih struktur še v fazi izdelave, oz. priprave. V prispevku najprej opišemo osnovne lastnosti sinhrotronske svetlobe, podamo pregled glavnih eksperimentalnih metod, kjer uporabljamo sinhrotronsko svetlobo in komentiramo, kako lahko sinhrotronsko svetlobo uporabimo za izdelavo mikro komponent. Na koncu bolj podrobno predstavimo predvideno slovensko žarkovno linijo BOSS pri novem izvoru sinhrotronske svetlobe ELETTRA, ki je zgrajen blizu Trsta.

1. Introduction

Synchrotron radiation became available in a routine manner to the scientific community in the early 1980s. Since that time the use of techniques employing synchrotron radiation has proliferated, so that its unique properties are now having a major impact on many areas of natural and technical sciences such as chemistry, material science, physics, biology, biochemistry, pharmacology, ecology, medicine, etc. /1-4/. Not only have new opportunities with existing methodologies been opened up but also several new techniques have become available. It is interesting to note that synchrotron radiation was first generated in the bending magnets of accelerators built for high energy particle physics research and that it took ten years before it was considered a potentially useful research tool instead of a mere technical nuisance for accelerator builders /5/.

Particle physics accelerators were soon inadequate to meet the demand for synchrotron radiation which was increasing within the scientific community. Dedicated storage rings and associated instrumentation with enhanced performance characteristics were then constructed in Europe, Asia and the USA (second generation sources).

During this period it became apparent that the brilliance of a source could be tremendously increased by introducing magnetic insertion devices in the storage ring (undulators and wigglers). The results were such that third generation sources, based essentially on insertion devices, were proposed in various places.

Third generation synchrotron radiation sources are characterised in general by an increased emphasis on the quality of the photon beam, expressed in terms of its spectral brightness, i.e. the number of photons emitted per second in a unit of the solid angle, source surface, and frequency bandwidth. High spectral brightness requires therefore a high photon beam intensity, a narrow spectral distribution and ease of focusing onto a small spot.

From the accelerator designer point of view, this implies a low emittance of the electron beam. This condition requires a strong focusing electron optics /6/. A strong focusing optics has the disadvantage of requiring strong chromaticity correction sextupoles and increased sensitivity to quadrupole misalignment and movement, which lead to short beam lifetimes and movements of the photon source. The challenge of the new generation of light sources is that the same optics characteristics that produce a high-brightness photon beam also make it difficult to obtain stable and reproducible operating conditions.

2. The Properties of Synchrotron Light

The main advantages of synchrotron radiation over conventional sources (X-ray tubes and UV lamps) can be summarised as:

- analytic computability of the source properties
- broad and continuous spectrum without peaks and dips
- high flux
- small divergence
- high brilliance
- pulsed operation for time-resolved studies
- highly polarised
- very stable and reproducible source
- UHV clean source for surface analysis - no gases, no plasma

2.1 Radiation of a single charged particle

Synchrotron radiation, which is electromagnetic radiation emitted during the transverse acceleration of charged high energy particles /7-10/ (electrons and positrons), got its name because it has been first seen at a synchrotron /11/. When the high energy particles pass into the magnetic field of the bending magnet they deviate and emit light tangentially to the curve /12/. The radiation emitted has the shape of a fan with an opening angle of the order $1/\gamma$ where γ is the relativistic Lorentz factor:

$$\gamma = \left(1 - v^2 / c^2\right)^{-1/2}$$

which is proportional to the electron energy $E = mc^2\gamma$

The total power emitted scales with the fourth power of γ and is inversely proportional to the second power of the electron's radius of curvature ρ:

$$P = \frac{e^2 c\, \gamma^4}{6\pi\varepsilon_0\, \rho^2}$$

with e being the electron charge. The power is continuously distributed over the frequency spectrum such that the so-called critical frequency

$$\omega_c = \frac{3c\, \gamma^3}{2\rho}$$

divides the total power spectrum into two equal parts. For a synchrotron light source with $E = 2$ GeV ($\gamma \approx 4000$), $\rho = 5.5$ m, the critical frequency and the corresponding critical wavelength $\lambda_C = 2\pi c/\omega_C$, respectively, belong to the X-ray domain: $\lambda_C = 0.38$ nm.

For the soft X-ray and ultraviolet range, an energy of 2 GeV is sufficient and such third generation sources are built on a national scale (BESSY II - Germany, ELETTRA - Italy, ALS - USA, Pohang - Korea, SRRC - Taiwan). To achieve wavelengths of several hundredths of a nanometer higher energy is required. Three hard X-ray facilities are under construction or in operation: SPring8 (Japan - 8 GeV), APS (Argonne/USA - 7 GeV), ESRF (Grenoble/France - 6 GeV). In the case of the ESRF, European co-operation was needed for the construction of such a facility in view of its complexity, cost and experimental potential.

2.2 Insertion devices

In the new light sources the most important elements are the magnetic systems, called insertion devices/13/, inserted in the straight sections of the storage ring. There are two types of insertion devices: wigglers and undulators. Each comprises a succession of small magnets of alternating polarity (figure 1) producing a vertical component of the magnetic field as $B_x(s) = B_0 \cos(2\pi s/\lambda_u)$ with s being the longitudinal co-ordinate and λ_u the period of the magnetic structure.

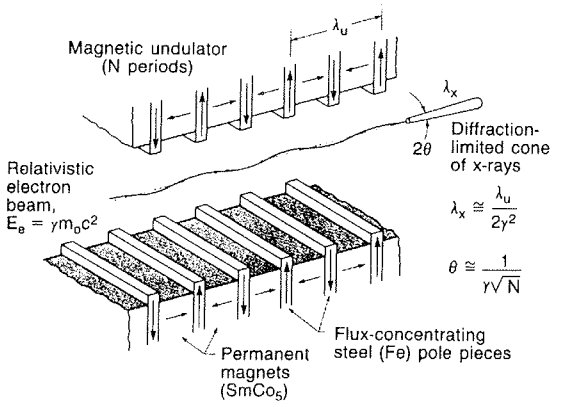

Fig. 1: Schematic of a periodic magnet structure (an undulator). The amplitude of the electron trajectory and the light cone size are not to scale.

The resulting magnetic fields force the electrons to oscillate around a linear trajectory. The light cones emitted at each bend superimpose and in the case of the wigglers their intensity increases proportionally to the number of bends while the spectrum is still continuous.

In the undulators the deviations are weaker, thus the light cones from the different bends overlap and at wavelengths given by /14/

$$\lambda_x \approx \frac{\lambda_u}{2\gamma^2}\left(1+K^2/2\right)$$

the interference effects produce a spectrum with a brilliance increased by the square of the number of bends. This radiation has peaks at odd multiples of λ_X and has a spectral width of $\lambda_X/\Delta\lambda_X \approx 1/N$, N being the number of undulator periods (figure 2). The dimensionless variable $K = 0.934\ B_0$ [T] λ_u[cm] is a measure for the type of insertion device ($K >> 1$ for wigglers and $K \leq 1$ for undulators).The magnets on the undulator are mounted on two jaws that can be opened or closed as required in order to change the on-axis magnetic field B_0 and in turn the value of K. Thus the wavelength maxima λ_X of the radiation emitted by the undulator can be shifted over part of the spectrum. The spectral brilliance of a typical rotating anode X-ray source is only around 10^7 photons/s/mm^2/mrad^2/(0.1% bandwidth), while the best synchrotron sources reach 10^{19} and more.

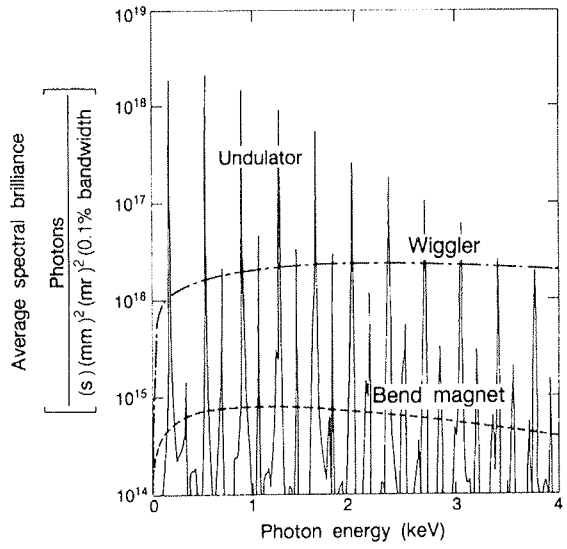

Fig.2: Harmonic content of undulator radiation arising from interference of radiation from different undulator periods (full line) compared to the spectrum of wiggler (dash-dotted) and bending magnet (dashed) radiation for the ALS /15/.

3. EXPERIMENTAL METHODS

Only a brief overview of the main experimental methods with synchrotron light is presented here. The reader is encouraged to read the exhaustive overviews in references /1-4/.

3.1 X-ray Absorption Spectroscopy

X-ray Absorption Spectroscopy (XAS) is ideally suited to probe the immediate environment of specific atoms. An X-ray absorption spectrum is usually divided, for convenience of interpretation, into three regions: the pre-edge and edge; the X-ray absorption near edge structure (XANES); the extended X-ray absorption fine structure (EXAFS).

The excitation of a core electron into the continuum may be convoluted with transitions from the core level to outer bound states resulting in features in the absorption spectrum that precede the absorption edge. The position and intensity of such features are dependent upon the electronic structure and the local symmetry at the primary absorber as the atomic transition is forbidden by the $\Delta l = \pm 1$ selection rule. Valuable structural insights may be obtained from the nature of such effects. The chemical shift in the absorption edge is a measure of the net charge on the primary absorber and, therefore, can serve as an indicator of the element's oxidation state.

The spectral features of XANES and EXAFS arise as a consequence of local electron diffraction. The principal distinction between XANES and EXAFS is that the former invariably involves multiple scattering of the photoelectron within the cluster of atom surrounding the primary absorber, whereas the latter usually does not. The XANES is therefore difficult to interpret, making it an empirical, although very sensitive, fingerprint of the immediate environment about the primary absorber. Direct comparisons of measured spectra can prove extremely useful.

First discovered in the 1930s /16/, the interpretation of EXAFS has progressed from the plain wave, single scattering approximation, to a full spherical wave treatment /17/ which allows the inclusion of multiple scattering pathways. Analytical procedures in k-space involve simulations of EXAFS profiles and refinement of structural and other parameters to produce the optimum agreement between the theoretical and measured data as described in /18/.

The structural parameters available from EXAFS analysis are the distance, the occupation number and Debye-Waller parameter for the nearest and possibly next-to-nearest shell of atoms around the primary absorber (up to an atomic distance of 0.3 - 0.5 nm). Careful modelling of the measured data can also reveal the atomic number Z of the neighbouring atoms.

The simple correlation between EXAFS and the local atomic environment, which has been first pointed out in /19/, is extremely important. Unlike X-ray diffraction, which collects information simultaneously on a large number of atoms in the system and is therefore extremely non-local in nature, the EXAFS is not limited to systems with long-range order. The technique is therefore unique for the study of the chemical structure of amorphous solids, liquids, solutions and gases. Also, since the EXAFS spectrum is measured on a known absorption edge, due to an atom of known chemical

type, the technique is chemically specific, giving the co-ordination of a known type of atom.

If, instead of measuring the absorption directly, the secondary process of X-ray fluorescence is monitored /20/, a considerable improvement in the spectral quality of low concentration atoms is achieved, pushing the sensitivity of the EXAFS technique to the levels necessary for the detection of diluted impurities /21/. The same method is also applied for thick samples, where the transmitted X-ray intensity is too low for a precise determination of the absorption coefficient.

Surface EXAFS (SEXAFS) is the surface-sensitive version of the EXAFS technique which implies the use of a surface-sensitive detection method. One of the possibilities is to measure the yield of secondary electrons /22/, because they have a mean free path in the sample between 0.5 and 5 nm, depending on their energy. By tuning the position in energy of the detecting window, one can, in principle, obtain layer-by-layer information on the local atomic structure. This method can be made atomic-species selective on the cost of losing depth tunability by tuning onto the energy of the Auger electrons produced by the core-hole recombination as pioneered in /23/.

3.2 X-ray Standing Wave

X-ray standing waves occur parallel to the surface of a crystal when the incoming and the Bragg reflected waves interfere. At normal incidence of the primary beam, the reflection curve has a wide range, therefore the effect takes place also in less perfect crystals. This opens the possibility to perform XSW on a wide range of materials.

When the photon energy is scanned through the region of a Bragg reflection, the standing wave outside the surface will move. This is equivalent to rotating the sample, as in measurement of the crystal rocking curve.

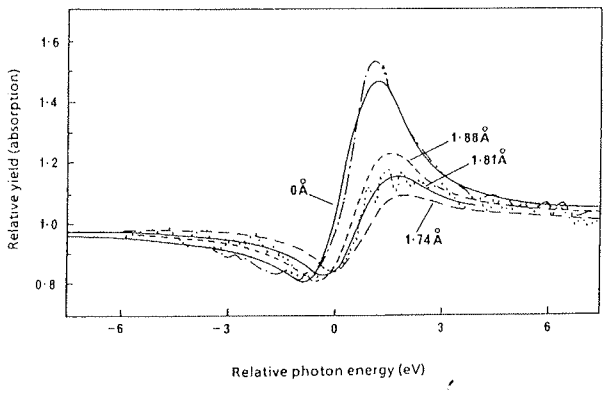

Figure 3: Experimental copper (-.-.-) and chlorine (...) Auger electron yields as a function of photon energy around the normal incidence [111] Bragg reflection. The theoretical curves are calculated for different plane spacing, showing that copper coincides with the surface and that the chlorine layer is 1.81 Å above the surface.

As the node passes through the position of adsorbed atoms, the characteristic Auger electron or fluorescence signal from these atoms will go through a minimum, while an antinode will produce a maximum. Thus the vertical distance of the adsorbate layer can be determined to a precision of a few pm, even at very low adsorbate concentrations, down to a few percent surface coverage. An example is shown in figure 3 for a regular overlayer of chlorine atoms on a Cu[111] surface /24/. This technique actually measures the spacing of the overlayer atoms from a continuation of the perfect bulk lattice rather than from the real surface layer, which may be relaxed or reconstructed in some way. By measuring XSW on two or more lattice planes, the exact position of the adsorbed atoms with respect to the substrate atoms can be determined through simple triangulation.

To have diffraction at normal incidence with low index Miller planes, a range in energy between 2 and 6 keV is necessary. The experiments are quite simple involving only a scan in energy of the incoming radiation instead of a scan in angle. However, the required monochromator resolving power is about 5000. Since SEXAFS and XSW can use the same beam line and the same experimental apparatus, this is a natural combination of methods for determining surface adsorbate geometries.

3.3 X-ray Fluorescence Spectroscopy

Fluorescence X-rays occur when an electron of a higher atomic shell decays into the previously emptied core level and releases its energy.

The characteristic energy of the fluorescence X-rays, different for each chemical element, makes X-ray fluorescence spectroscopy (XRF) a very suitable method for the detection of elements in very low concentrations. Several methods exist that allow to determine concentrations of major, minor and trace elements from the fluorescence yield, either by using reference standards or based on fundamental parameters /25/.

The following characteristics of synchrotron radiation besides the obvious high incident X-ray flux available are exploited for XRF trace element analysis in order to achieve the lowest possible detection limit:

- the tunability of the excitation energy offers the possibility of obtaining the highest sensitivity throughout the whole range of elements of interest by tuning the excitation energy just above the binding energy of the electrons in a particular shell of the element of interest;
- the linear polarisation of the synchrotron beam enables a low background to be achieved, in particular if the fluorescence X-rays are detected at 90° to the incident radiation where no Compton scattering occurs.

Compared with ion-bombardment, the radiation damage induced in the specimen under investigation is considerably less. Especially for biological applications this is a major advantage. Moreover, one can perform

XRF measurements in air or under a protective atmosphere instead of the vacuum necessary for ions.

Because of the high flux available, a wavelength dispersive detector with a higher resolution and thus a better signal/noise ration can be used instead of the more common solid state energy dispersive detector. The lowest detection limit depends very much on the element and the underlying matrix, however, detection limits as low as a few parts /26/ to a few tens of parts /27/ per billion have been reported.

If the photon beam impinges on the sample at angles below the critical one, total reflection occurs. The penetration depth is very small resulting in a good surface sensitivity and in a complete suppression of the scattering background in the fluorescence spectrum. The total reflection XRF method was successfully explored using X-ray tubes /28/, nevertheless up to now the full potential of this method has not been exploited at synchrotron radiation sources yet.

3.4 Electron Photoemission Spectroscopy

Since electrons have a mean free path of only a few atomic diameters in the energy range of 50 - 1500 eV, a number of particle-based techniques are surface sensitive such a low energy electron diffraction (LEED), Auger electron spectroscopy (AES), high resolution electron energy loss spectroscopy (HREELS) and others.

For photoelectron spectroscopy with a synchrotron light source, major advantages arise from the tunability, polarisation and brightness of the source. Tunability allows to optimise surface sensitivity by maximising cross-section and by gearing the kinetic energy of the emitted electron to the minimum escape depth. The polarised nature of the source allows the symmetry of electron states in the surface to be determined.

Here, only one striking example is shown in which the tunability of the source may be exploited to yield interesting information. For instance, figure 4 shows the photoemission yield from amorphous metallic glasses of $Cu_{30}Zr_{70}$ and $Cu_{40}Zr_{60}$ measured at two different photon energies /29/. The valence bands comprise a mixture of states derived from Cu 3d and Zr 4d orbitals. The former exhibit a fairly smooth variation in cross-section as the energy is varied but the 4d states, with a node in their wave function, change in intensity by about two orders of magnitude in the range chosen, allowing easy separation of the contributions to the valence band, with the Zr states found to be near the Fermi level (E=0) and thus dominating the conductivity.

Another powerful method is the measurement of core level shifts. The binding energies of core level electron states are sensitive to the valence level environment of the atom. The corresponding chemical shifts of the core level energies of adatoms, typically by several electron volts, are used to monitor the presence of different valence states on surfaces. This is the basis of the familiar use of ESCA (electron spectroscopy for chemical analysis) which has been pioneered by K. Siegbahn /30/. More recently, using high resolution instrumentation, core level shifts of substrate atoms has been measured, and favourable circumstances, it has proved possible to use this technique to distinguish surface substrate atoms from bulk atoms and even from atoms on intermediate layers (figure 5) /31/. The shifts here

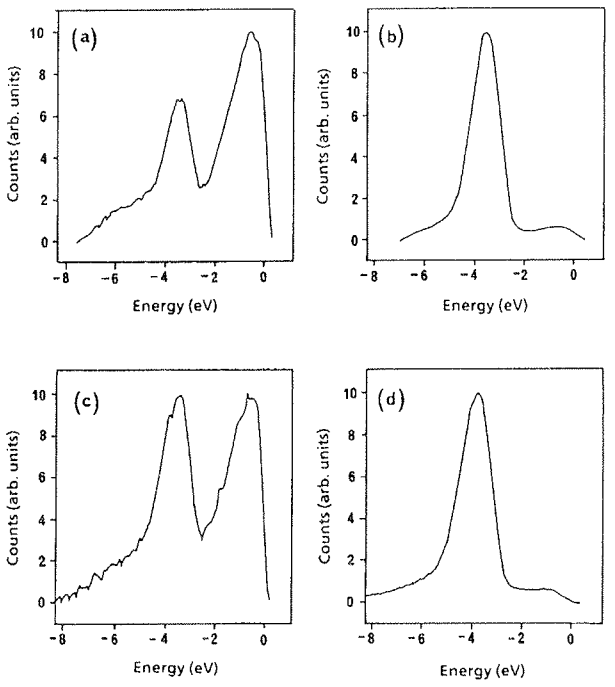

Fig. 4: Photoemission spectra of (a), (b) $Cu_{30}Zr_{70}$ and (c), (d) $Cu_{40}Zr_{60}$ at photon energies of (a), (c) 40 eV and (b), (d) 120 eV.

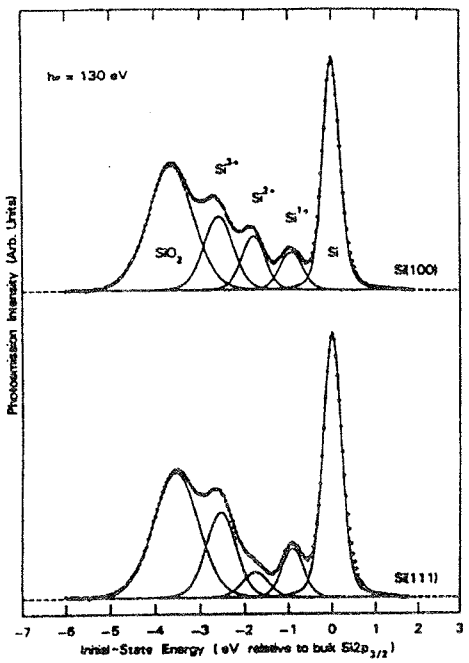

Fig. 5: The Si $2p_{3/2}$ components of Si 2p spectra from thin oxide films of approximately 0.5 nm thickness thermally grown on Si(100) and Si(111) surfaces. Note the reduced intensity of Si^{2+} for Si(111), assumed to be due to structural differences in the interface.

arise from the difference in co-ordination of surface atoms and bulk atoms. This narrows the valence band, which is shifted in energy in order to maintain charge neutrality at the surface. A similar shift is observed by all the core levels. Further shifts are also induced by charge transfer to or from chemisorbed atoms, and surface core level shifts thus provide a useful tool for the characterisation of adsorption sites.

Even more powerful experiments include the measurement of the photoelectron angular distribution. Those methods include angle-resolved photoemission, photoelectron diffraction, Auger electron diffraction and photoelectron holography /32/, which can actually give the position and orientation of single adatoms on surfaces.

3.5 X-ray Diffraction

For decades, elastic X-ray scattering techniques have been the leading probe of the geometric micro structure of molecules and solids. They can be divided into two broad areas. Experiments in the first area (wide angle X-ray scattering - WAXS) investigate systems with long-range order such as single crystals. The second area (small angle X-ray scattering - SAXS) investigates disordered systems, such as liquid solutions and alloys, and partially ordered systems like fibrous biological specimens, liquid crystals, polymers, and others.

Wide angle scattering from crystalline material, i.e. diffraction, is most simply described in terms of the Laue equations, the solutions to which are given by $\Delta\mathbf{K} = \mathbf{G}$, where **G** is a vector of the reciprocal lattice and $\Delta\mathbf{K}$ is the scattering vector, i.e. the difference between the wave vectors of the incident and scattered radiation. Each diffracted beam corresponds, in reciprocal space, to the scattering vector touching a reciprocal lattice point. From the positions of the scattering peaks, therefore, one can in principle determine the crystal lattice.

The intensities of the peaks on the other hand are related - besides a dependence on the Debye-Waller factor - to the square of the structure factor containing the information on the electron density inside the unit cell. However, since the intensity is a scalar quantity, the phase of the complex structure factor is indeterminate - the basis of the well-known 'phase problem' in crystallography. Classically this has been approached using the technique of multiple isomorphous replacement (MIR) /33/.

The tunability of synchrotron radiation can be exploited for an alternative solution, based on the technique of multiple wavelength anomalous diffraction (MAD) /34/. The phenomenon arises from resonance effects due to the fact that core level electrons scatter differently from free electrons. As the elemental absorption edge is approached, the atomic scattering factor of that element becomes complex and varies rapidly unlike in the case of Thompson scattering. The net intensity of each Bragg reflection is then energy or wavelength dependent and this variation may be used to solve the problem in a manner analogous to, but without the inherent problems of, the MIR method.

X-ray scattering is so powerful in the determination of crystal structures, because the wavelength of the radiation is comparable to inter atomic distances. Measurements of larger structures in principle needs radiation of longer wavelength. However, the electromagnetic spectrum between 1 and 100 nm is unsuitable for scattering techniques because of strong absorption. Structures of these dimensions can therefore only be studied using X-rays scattered at small angles. SAXS provides information on the overall shape and size of the scattering objects, its density, orientation, packing with other objects, etc. Since X-ray scattering arises from electron density fluctuations in the specimen, a scattering object can be any inhomogeneity - a molecule in solution, a small crystal, a part of a large molecule, a solid or a liquid particle, and so on.

The interpretation of SAXS measurements depends on models for individual types of specimen. The most common parameters are obtained from the plot of scattered intensity I versus magnitude of the scattering vector q. From Guiner's Law /35/, valid in the low angle region, the radius of gyration of the scatterer is obtained. The limit of large q is described by Porod's Law /36/ revealing the mean square electron density fluctuation, which is determined by the periodicity of the system. In case of aggregated systems, the region in between is directly related to the fractal dimension of the system.

The ability to perform anomalous dispersion studies is important also for SAXS measurements. It is especially valuable for disordered materials, because in that case anomalous dispersion directly allows to distinguish con-

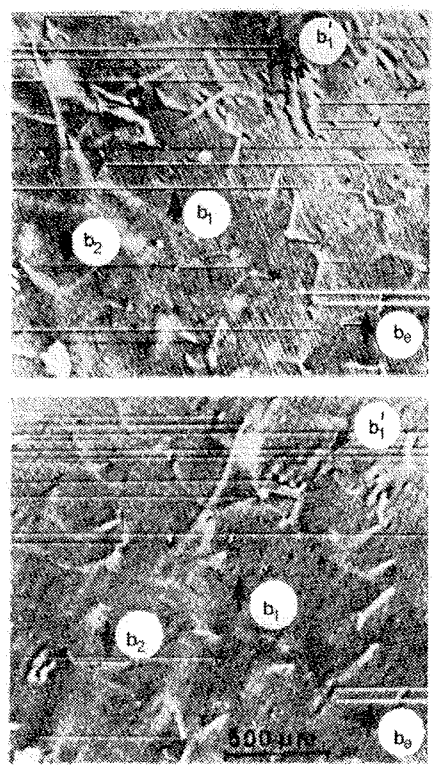

Fig. 6: Epitaxial dislocations in $Ga_{1-x}Al_xAs_{1-y}P_y$ / GaAs heterojunctions (after /37/). Indicated are the Burger vectors.

tributions from different types of atoms to the scattering intensity, without having to refer to models.

X-ray topography is a subfield of X-ray diffraction which produces two-dimensional maps of crystal distortions /37/. The intensity of a Bragg reflection changes when the crystal is distorted. By monitoring the intensity of a Bragg reflection in different points of the crystal, one can create a two-dimensional map of its distortions (see figure 6). This topographic method is very powerful in the study of imperfect crystals and overlayers with technological interest. X-ray topography has a spatial resolution of several micrometers which is much worse than that of dark field transmission electron microscopy. However, due to the low absorption of X-rays, fairly massive single crystals may be imaged and X-ray imaging techniques are characterised by a unique strain sensitivity, down to 10^{-8}.

4. PRODUCTION WITH SYNCHROTRON LIGHT

Although synchrotron light has been mainly used as a source of photons for analytical purposes, the radiation can be also used to induce chemical reactions and thus produce structures just like in normal photo chemistry. Due to the short wavelength of the radiation, it is particularly suited for micro fabrication. Two most prominent applications are the production of integrated circuits on the micro- and nanoscale with X-ray lithography and the production of micro- and nanomechanic devices by means of the Liga method.

4.1 Lithography

Since the early 1980s it has been predicted that the limit in the spatial resolution of conventional fabrication has been reached and that the next generation of integrated circuits will have to be produced with synchrotron sources. X-ray lithography with synchrotron radiation has proved to be a valuable technique in the laboratory and can sustain comparison with deep-UV lithography and electron beam lithography regarding resolution, wafer throughput and process latitude. However, the conventional techniques have been improved constantly and there are only a few dedicated X-ray lithography light sources at major companies in Japan (NTT, Mitsubishi and Sumimoto) /38-39/ and one system at IBM's plant in Fishkill /40/, which was constructed by Oxford Instruments /41/. The transfer of synchrotron radiation lithography technologies to an industrial production environment just involves considerable problems that have yet to be overcome in order to be acceptable by the industry. If we are to believe current estimates /42/, then it will become a major technique in the year 2001 when UV techniques will reach their final limit.

The main limitation of the micro lithography process based on ultraviolet radiation exposure is caused by diffraction. The intrinsic diffraction limit in reproducing narrow features of the mask is approximately equal to the wavelength of the radiation. A typical photon source for UV lithography is the intense mercury line at 365 nm, although weaker sources exist at smaller wavelengths of 230 - 300 nm. The spatial resolution can be improved by using suitable demagnifying lenses. However, these lenses have a short depth of focus, i.e., they require very flat silicon wafers. Another serious problem are dust particles, which are strong scatterers of UV radiation in the above range.

These factors make it desirable to use radiation of shorter wavelengths. Besides removing the diffraction problem, shorter wavelength photons have the additional advantage of being less sensitive to dust than UV radiation. X-ray lithography can be in principle implemented with conventional sources, e.g. stationary anode sources and laser-induced plasma sources.

A synchrotron radiation source offers clear advantages /43/. The first one is the intensity of the synchrotron radiation source. This shortens the exposure time of each wafer and decreases the production costs. A second advantage is the small source size, which reduces the penumbra effect (figure 7a). The penumbra effect can be reduced also by placing the source far from the mask. This is easily achievable due to the third advantage of synchrotron radiation, namely the small divergence. The same considerations apply to another problem, illustrated in figure 7b. This is the geometrical distortion due to the different angle of incidence of a divergent X-ray beam in different areas of the mask. The technical term for this problem is "run-out". Once again, the small angular divergence of synchrotron radiation is extremely helpful in removing this problem.

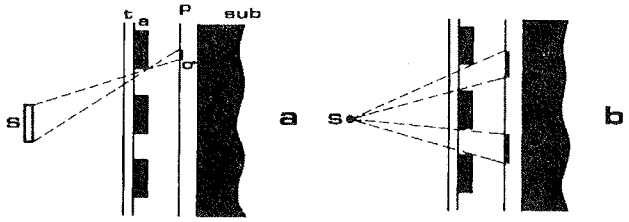

Fig. 7: Two problems affecting X-ray lithography with conventional sources: a) the finite size of the source causes penumbra effects, with an edge blurring corresponding to the area s and b) the divergence of the source causes distortions of the transferred pattern. s - source, t - transmitting substrate, a - absorbing pattern, p - photoresist, sub - substrate.

Currently the most developed technique in terms of R&D is the so-called X-ray proximity lithography (XRL), where a mask with a patterned absorber is placed in close proximity (<50 μm) to a resist-coated substrate. New chemically amplified resists of high sensitivity (30-100 mJ/cm^2) and high resolution (0.1 μm) are commercially available /44/. X-ray steppers are also manufactured with an overlay performance in 3σ of 70-90 nm /45/ and have been used for device fabrication. High performance SRAMs in a 0.25 μm CMOS technology have been fabricated by IBM /46/. The NTT (Japan) program is also aimed at 0.25 μm CMOS /47/ and it is

expected that the XRL technology can be pushed down to 0.1 μm or even 50 nm. Currently, the mask technology remains the key point to insure the complete success of XRL. It has been considerably improved in the last decade, but further improvements are still necessary.

An X-ray mask consists of a transparent flat membrane supporting opaque absorber structures. Membranes are formed by the deposition or growth on a silicon wafer. Their thickness must not exceed 3 μm in order to get enough X-ray transmission. Many materials have been studied in the last decade, as they have to meet a number of relevant properties: low roughness, flatness, robustness, high fracture strength, stiffness, stability under irradiation, large thermal conductivity, low thermal expansion coefficient, and visible optical transparency. Today, B doped Si /48/ are the most widely used in the US, while SiN_x is the current standard in Japan /49/. The best materials for future membranes seem to be SiC and diamond, but there is still some development to be done. The absorber is a high atomic weight material. Currently, Gold, Tungsten and Tantalum are the most used ones. The mask patterning is realised by a focused electron beam system with electron energies from 50 to 100 keV.

X-ray lithography does not require a high-resolution monochromator to filter the radiation emitted by the synchrotron radiation source. A wide band of wavelengths is typically used, since this increase s the total power reaching the wafer and decreases the exposure time. However, the exposing wavelength must be compatible with a relative good absorption in a resist film (i.e. 10-50% in a thickness of 1 μm), minimised diffraction effects and easy mask technology. This last requirement implies a reasonable transmission through the mask membrane (50-90%) and reasonable attenuation in an absorber for a film thickness no more than 4 times the minimum feature size. This fixes the optimum spectral range for XRL between 0.8 and 1.5 nm.

4.2 Liga

Three-dimensional microscale structures can be fabricated with the Liga process, which uses deep etch X-ray lithography, electroforming and plastic moulding. Development of the Liga process began at the Karlsruhe Nuclear Research Centre (KfK) in the late 1970s as an inexpensive method of producing very small slotted nozzles of any lateral shape for uranium isotope separation /50/. Liga is a German abbreviation of the three major process steps: lithography (Lithographie), electroplating (Galvanoformung) and moulding (Abformung).

A schematic diagram of the steps involved in fabrication of basic Liga microscale structures is shown in figure 8. In the first step the absorber pattern of an X-ray mask is transferred into a resist layer several hundred micrometers in thickness by X-ray shadow projection. Synchrotron radiation is used because of its very high collimation and short wavelength. The range used extends from 0.2 to 10 nm. The X-ray masks consist of a thin membrane (e.g. 3 μm titanium or 30 μm beryllium) together with absorbers consisting of gold layers that

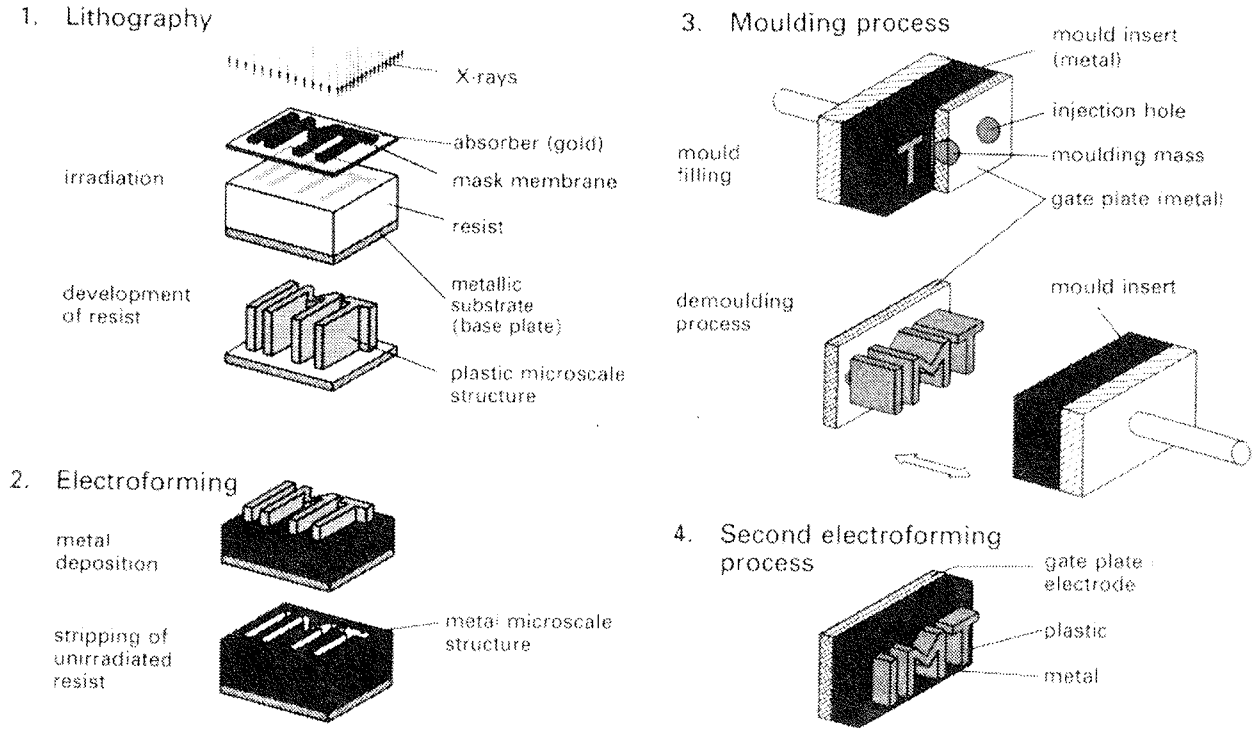

Fig. 8: The principal process steps for fabrication of microscale structures by the Liga technology.

are thicker than 10 μm in order to achieve the required mask contrast. Within the irradiated sections of the resist layer the polymer chains are destroyed, reducing the molecular weight. In most cases polymethylmethacrylate (PMMA) is used as the X-ray resist. During the subsequent development step, the exposed resist is selectively dissolved while the unirradiated parts remain unchanged. The unexposed regions of the resist, covered during irradiation by the absorbers of the mask, form the primary microscale structure.

Electrodeposition on a microscale can then be employed to build up a complementary pattern in a metal such as copper, nickel or gold, by filling the empty spaces of the electrically non-conducting resist. The metal pattern produced in this way can then be used to manufacture, with a high degree of detail and at relatively low cost, almost any number of plastic copies by means of moulding processes such as reaction injection moulding, thermoplastic injection moulding and hot embossing of thermoplastics.

The latter is particularly suitable for moulding microscale structures on processed silicon wafers, e.g. on microelectronic circuits /51/.The wafer, already carrying the protection and metallised layers, is laminated with the moulding compound. In the next step the wafer and the plastic material are heated and an evacuated mould insert is pressed into the moulding compound. Once the compound has cooled the mould insert is removed. A wide variety of plastic materials can be patterned by these moulding techniques, including PMMA, polycarbonate, polyamide, polyethersulfone, polyoxymethylene, polyvinylidene fluoride and epoxy resin.

The plastic structures can again be filled with metal in a second electroforming process. Therefore, metallic microscale structures can also be fabricated in a cost effective way. As an example, in figure 9a a micro mesh honeycomb structure made of nickel is shown, which was built up on a processed silicon wafer by the embossing and electroforming technique.

In order to obtain partly or totally movable microscale structures together with fixed structures on a single substrate, a integrated fabrication technology, based on a sacrificial layer technique, has been developed /52/. The substrate is first coated by physical vapour deposition with a thin (<1 μm) metallic layer, which is patterned by photolithography and wet etching. This layer serves both as a plating base and as an electrically conducting level for the finished structures. In the second step a sacrificial layer, about 5 μm in thickness, is deposited on the substrate and also patterned by the same methods. Titanium is used as sacrificial material because it adheres well to the resist and to the electrodeposited layer and can be etched with hydrofluoric acid which does not attack the materials (chromium, silver, nickel, copper) usually used in the Liga process.

The standard Liga process is then used: polymerisation of the thick X-ray resist directly on to the substrate, exposure to synchrotron radiation through a precisely adjusted mask, development of the resist and electrodeposition. Some parts of the metallic microscale structures will be built up on the first metal layer, while other parts lie on top of the sacrificial layer. After stripping the resist, the sacrificial layer is etched selectively against all other materials, exposing some parts of the micro structure.

With the techniques described above, the Liga process may be used to fabricate microscale structures of any lateral shape and with the following characteristics:

- structural heights up to and greater than 1 mm
- edge details less than 0.25 μm in dimensions
- lateral dimensions of the order of a few micrometers
- sub micrometer accuracy over the total height of the structure.

New process steps /53/ permit even a variation of the geometry in the third dimension in order to produce stepped structures and structures with inclined sidewalls. One of the most novel features of the Liga process is the wide variety of materials that may be used, including plastics, metals, alloys and ceramics.

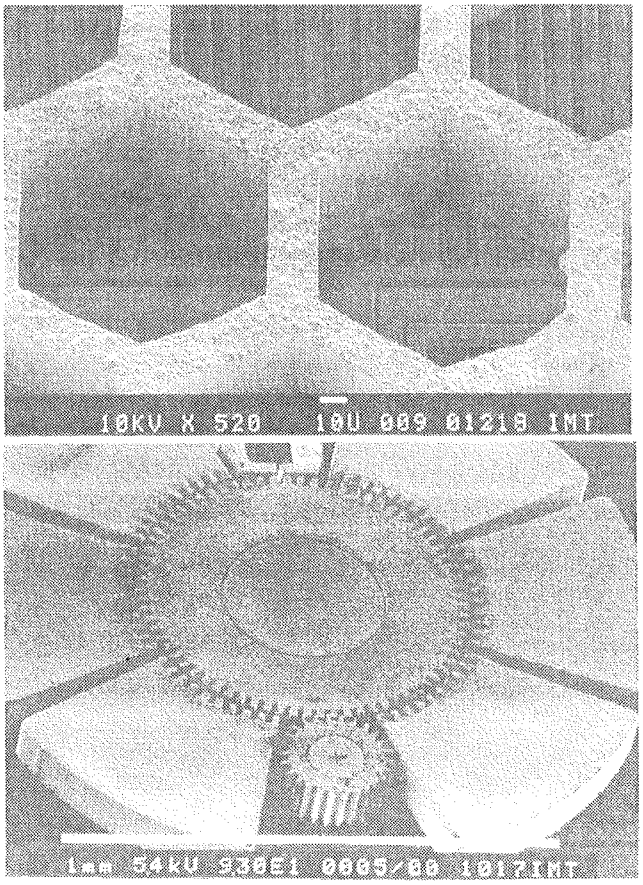

Fig. 9: Two examples of microfabricatrion with Liga: a) Nickel honeycomb structure fabricated on processed silicon wafer by the hot embossing technique and the electroforming process: width of walls 8 μm, height 100 μm; b) Electrostatic nickel micromotor with toothed rotor (dia. 700 μm) and stators, gear wheel (dia. 250 μm) for torque transmission and fixing groove for optical fibre to allow speed measurement: gaps between rotor and axle and rotor and stators 4 μm, height 120 μm.

A list of movable micro structures produced include physical sensors and actuators, such as acceleration sensors, turbines, linear electromotors, circular electromotors (figure 9b) and pumps. /54/. Numerous further microscale structures are under development, for example: micro coils, ultrasonic sensors, electrostatic linear actuators, springs and micro optical components /55/ which are used for optical communication technology and fibre optical sensing. In future, the combination of Liga process technology with other micro fabrication techniques such as anisotropic etching of silicon or reactive ion etching will greatly expand the number of applications by taking advantage of the special benefits provided by these individual technologies. Particularly promising are medical applications for minimal invasive therapy where lies the greatest interest for micro structures .

5. THE SYNCHROTRON LIGHT SOURCE ELETTRA

The Trieste synchrotron light source ELETTRA /56/ is the world's brightest light source in the UV and soft X-ray region. As such it further extends the possibilities of research with respect to existing light sources. The storage ring operates at an energy of 2 GeV with an electron current of 200 mA, to be increased to 400 mA in a later phase. The total circumference of the machine with 24 bending magnets is 260 m. Eleven straight sections can be equipped with 4.5 m long insertion devices, each feeding two beamlines. A wiggler can serve two beamlines simultaneously, while the light cone from an undulator is too small to be split in two. Therefore, a switching mirror distributes the light between the two attached beamlines. In addition, 13 bending magnets may be used as light sources for experiments with 2 beamlines per magnet. Over 25 beamlines have been proposed up to now, out of which 8 are already in operation or in the phase of commissioning (table 1). The first official operation run with experiments that have been selected from proposals through an international scientific review committee has started recently (August 30-th).

6. THE BEAM LINE BOSS

Triggered by the proximity of this excellent source, researchers in Slovenia have established the collaboration BOSS (Beam line Of Slovenian Scientists) which seeks ways to perform research at ELETTRA and to construct the beam line BOSS.

Since the beam line BOSS is a national project, it has to allow as many experiments as possible to researchers from Slovenia, as long as they can be reasonably well performed on BOSS, even though some fields may be covered by other beamlines. Hence BOSS is a multipurpose beam line, employing the following experimental methods: XAS (X-ray absorption spectroscopy, i.e. XANES - X-ray absorption near edge structure and EXAFS - extended X-ray absorption structure), XRF (X-ray fluorescence) and XPS (X-ray photoelectron spectroscopy), with the possible extension to WAXS (wide angle X-ray scattering), SAXS (small angle X-ray scattering) and XSW (X-ray standing wave).

*Table 1: The main characteristics of the beamlines currently or shortly in operation. The last two (marked with an asterix *) employ special focusing optics such that the photon beam size is only 50 nm. The photon spectral flux in this spot is of the order of 10^9 photons/s/0.1%b.w. . The other beamlines have beam sizes around 0.1 - 1 mm and have fluxes in the range from 10^{12} - 10^{14} photons/s/0.1%b.w. .*

Name	Eph [keV]	resolution	experiments
SuperESCA	0.1 - 2	10000	high resolution and/or high flux ESCA; photoelectron diffraction; studies of dynamic surface phenomena
VUV Photoemission	0.02 - 1.2	10000	semiconductor surfaces; interface formation; high-T superconductors; electronic structure of metals and their surfaces
ALOISA	0.25 - 8	5000	surface X-ray diffraction; photoelectron diffraction; coincidence experiments
Diffraction	5- 25	>1000	determination of macromolecular biological structures; studies of temporal variations of structures
SAXS	5.4, 8, 16	1000	material physics; polymer science; biomembranes
GasPhase Photoemission	0.02 - 1.2	12000	gas phase reactions of chemicals; chemistry of combustion; electronic structure of gas atoms and molecules
Spectromicroscopy*	0.02 - 0.8	3000	high lateral resolution photoemission, used for highly inhomogeneous solids, micro crystals, biological structures; study of localised bad-bending phenomena caused by imperfections in semiconductors
ESCA microscopy*	0.1 - 2	3000	high lateral core level photoemission for the same topics as above

A recent survey among research groups in Slovenia has shown that there is interest practically in all experimental methods that can be offered by ELETTRA. Fortunately, more than 70% of the requests can be fulfilled by a single beam line operating in the X-ray region between 2 and 12 keV. About two thirds of those want to utilise absorption spectroscopy, in particular EXAFS or one of its flavours (SEXAFS, fluorescence EXAFS).

The EXAFS spectroscopy is a particularly interesting method for the industry, too. An analysis of recent industrial use of the SRS at Daresbury /57/ shows that 47% percent of the use is allocated to experiments with EXAFS making it the most widely used method for industrial synchrotron radiation research.

The beam line BOSS has been therefore designed primarily for absorption spectroscopy, exploiting the high spectral flux and small source point of the ELETTRA bending magnet as compared to other X-ray sources. The spectral region covers either the K-edge or the L-edge of almost all elements between and including phosphorous (Z=15) and platinum (Z=78), giving sufficient tunability for a wide range of absorption experiments. The limits actually come from the absorption in the C and Be filters below 2 keV and from the poor reflectivity of the gold coated mirror above 12 keV /58/.

The expected characteristics of the beam line are a good photon energy resolution (3000 to 6000) in the range between 2 keV (0.62 nm) and 12 keV (0.1 nm), high spectral flux from a bending magnet source (about 10^{12} monochromatised photons/second over the whole spectral region), small focal spot size on the sample (below 1 mm^2) and a vertical divergence below 0.4 mrad /58/. These characteristics are probably sufficient also for XSW experiments, therefore XSW is considered as a potential method even though no proposals were submitted from Slovenian researchers yet.

The other two methods that have been requested by Slovenian research groups and are well suited to the characteristics of BOSS are fluorescence and photoelectron spectroscopy. None of them is covered by other beamlines at ELETTRA in the complete range between 2 and 12 keV. The main purpose of electron detection at BOSS is to allow total electron and Auger yield measurements for SEXAFS. However, the equipment can be set up in order to allow electron spectroscopy, too. The photon energy range of BOSS does not fall into the classical XPS region, although some useful spectra may be obtained at the lowest energy range from 2 - 3 keV.

Yet the higher photon energies could be efficiently exploited for some specific topics like:

- thick films, in particular buried interfaces, where the larger thickness forbids the penetration of low energy electrons to the surface
- the study of the change of the ratio between the main and satellite peaks between low and high energy photons, which is due to the difference between the adiabatic and sudden transitions.

Furthermore, the photoelectron spectra at these higher photon energies are relatively unexplored and it is always possible that new interesting phenomena could be observed. Therefore a thorough investigation of photoelectron spectra with BOSS might prove useful.

Photoelectron spectra obtained from BOSS are of interest also for atomic physics to study correlated processes in events with multiple photoelectron emission. Some proposed experiments include:

- Auger spectroscopy of satellite and hyper satellite lines;
- threshold spectroscopy for double K shell ionisation;
- Auger spectroscopy;
- determination of fluorescence yields and Coster-Kronig transition rates.

X-ray scattering already sees two dedicated beamlines at ELETTRA, the diffraction and the SAXS beam line (see table 1 above). However, the characteristics of BOSS allow also a range of scattering experiments and this can be exploited in order to allow Slovenian users immediate usage without having to wait for beam time at the dedicated lines. In addition, due to the fixed wavelengths of the SAXS beam line, BOSS is a possible candidate for anomalous SAXS experiments.

The main experimental chamber will be equipped to allow several types of measurements of the absorption coefficient, via the detection of the transmitted flux as well as the secondary processes like fluorescence, photoelectrons and Auger electrons. The chamber will allow the addition of particular sample chambers which will allow the study of crystalline, amorphous, liquid and gaseous samples under different temperatures, pressures and other physical and chemical conditions. Measurements of trace elements with XRF will be possible with the same chamber.

Other experiments will need a dedicated experimental chamber, such as surface science experiments, or dedicated detectors, such as atomic physics experiments, which is beyond the scope of the proposed project. However, the Slovenian beam line will deliver the proper type and quality of radiation. The chambers and specialised detectors will be constructed or are already under construction by individual users, like an energy and a wavelength dispersive X-ray spectrometer, an electron energy spectrometer, a four crystal monochromator, etc. Attachment ports for several kind of experimental chambers and detectors are foreseen.

For surface mapping, the addition of a glass capillary microprobe is envisaged, giving spatial resolution to all of the aforementioned methods of about 10 - 30 μm /59/ or even down to 1 μm /60/. For some cases the use of a PEEM (photoelectron emission microscope) camera is considered, giving a resolution of 0.5 μm and better /61/. A four crystal monochromator to be added after the mirror will provide a resolving power of 10000 whenever needed.

The scientific case, where 35 proposals from Slovenian research groups have been presented /62/, has been

recently approved by the Programme Advisory Committee of Sincrotrone Trieste. It is planned that once funds for the project become available, the beam line should be constructed in two years time.

7. CONCLUSIONS

Synchrotron radiation has proven to be a potentially powerful tool both for basic and applied research. The great success of the new third generation light sources has already triggered plans for other machines and even ideas for fourth generation machines. Maybe the only reason why many laboratory-based scientist have not used synchrotron radiation in their research yet, is the fact that synchrotron radiation is available only at large, centralised facilities.

However, the complexity and cost of modern experimental science is forcing experimenters to look for equipment that may not be available at the home laboratory. Some scientists may not like this trend, but it is a reality with which we must cope. Fortunately, due to the increasing supply of synchrotron radiation from all those sources and the construction of new national and regional sources (like Elettra) we can expect rapid expansion of research made with synchrotron light and - what is important for small groups - the continuation of free access both in financial and in scientific terms.

Whether synchrotron radiation will become the standard of industry based production of microelectronics and micro mechanics and whether all large IC producers will have their own compact synchrotron sources in their production plants still remains an open question. Technical problems notwithstanding, the feasibility of synchrotron radiation lithography has been clearly demonstrated in a number of prototypical production tests. It is definitely a challenging and highly expanding field.

8. ACKNOWLEDGEMENTS

The author expresses his sincere thanks to Iztok Arčon, who has done the detailed design of the BOSS beam line and to H.O. Moser, who has provided him with the newest information on the Liga process.

Special thanks go to all the colleagues from the Institute Jožef Stefan, the Universities of Ljubljana and Maribor and from the industry, who have submitted proposals and letters of support for the beam line and made the proposal a real project.

This work has been supported by the Slovenian Ministry of science and technology under contract J1-5057-0106/95.

9. References

/1/ Koch, E.E., editor, The Synchrotron Radiation Handbook, Vols. 1-3, North-Holland, Amsterdam (1983-1991).

/2/ Margaritondo, G., Introduction to Synchrotron Radiation, Oxford University Press, Oxford (1988).

/3/ Catlow, C.R.A. and Greaves, G.N., editors, Applications of Synchrotron Radiation, Blackie, London (1990).

/4/ Baruchel, J. et al., editors, Neutron and Synchrotron Radiation or Condensed Matter Studies, Vols 1-3, Les Editions de Physique, Les Ulis, France(1992-1994).

/5/ D.H. Tomboulian and P.L. Harman, Phys. Rev. 102, (1956) 1423.

/6/ D. Einfeld and M. Plesko, Nucl. Instr. Meth. Phys. Res. A335 (1993) 402-416.

/7/ D. Ivanenko and J. Pomeranchuk, Phys. Rev. 65, (1944) 343.

/8/ J. Schwinger, Phys. Rev. 70, (1946) 798.

/9/ D. Ivanenko and A.A. Sokolov, Dokl. Akad. Nauk. 59, (1948) 1551.

/10/ A.A. Sokolov and I.M Ternov, Dokl. Akad. Nauk. 92, (1953) 537.

/11/ F.R. Elder et al.,Phys. Rev. 71, (1947) 829.

/12/ J.D. Jackson, Classical Electrodynamics, Wiley 1962.

/13/ H. Winnick et al., Physics Today, May 1981.

/14/ S. Krinsky, M.L. Perlman, R.E. Watson in /1/, Vol. 1a.

/15/ 1-2 GeV SYNCHROTRON RADIATION SOURCE, Conceptual Design, July 1986, Lawrence Berkeley Laboratory, PUB-5172 Rev.

/16/ R. de L. Kronig, Z. Phys. 70 (1931) 317.

/17/ S.J. Gurman, N. Binsted and I. Ross, J. Phys. C 19 (1986) 1845.

/18/ Koningsberger, D.C., and Prins, R., editors, X-Ray Absorbtion, Principles, Applications, Techniques of EXAFS, SEXAFS and XANES, John Wiley & Sons, New York (1988).

/19/ D.E. Sayers, E.A. Stern and F.W. Lytle, Phys. Rev. Lett.. 27 (1971) 1207.

/20/ S.P. Cramer and R.A. Scott, Rev. Sci. Instrum. 52 (1981) 395.

/21/ F. Sette et al., Phys. Rev. Lett. 56 (1986) 2637.

/22/ J. Stöhr, D. Denley and P. Perfetti, Phys. Rev B18 (1978) 4132.

/23/ P.H. Citrin, P. Eisenberg and B.M. Kincaid, Phys. Rev. Lett. 36 (1976) 1346.

/24/ D.P. Woodruff et al., Surf. Sci. 195 (1988) 237.

/25/ R. Tertian and F. Claisse, Principles of Quantitative X-ray Analysis, Heyde, Hondon (1982).

/26 B.M. Gordon, Nucl. Instrum. Methods 204 (1982) 223.

/27/ W.J.M. Lenglet et al., Anal. Chim. Acta 173 (1985) 105.

/28/ W.C. Marra, P. Eisenberger and A.Y. Cho, J. Appl. Phys. 50(11) (1979) 6927.

/29/ D. Grieg et al., Mater. Sci. Eng. 99 (1988) 265.

/30/ K. Siegbahn, Rev. Mod. Phys. 54 (1965) 709.

/31/ F.J. Himpsel et al., Phys. Rev. B38 (1988) 6084.

/32/ C.S. Fadley, in Synchrotron Radiation research: Advances in Surface and Interface Science, Vol. 1, ed. R.Z. Bachrach, Plenum Press, New York 1992.

/33/ D.M. Blow and F.H.C. Crick, Acta Crystallogr. 12 (1959) 794.

/34/ Y. Okaya and R. Pepinsky, Proc. Natl. Acad. Sci. USA 42 (1957) 286.

/35/ A. Guiner and G. Fournet, in Small Angle Scattering of X-rays, John Wiley, New York, 1955.

/36/ G. Porod, Kolloid Z., 124 (1951) 89; 125 (1952) 51; 125 (1952) 109.

/37/ M. Sauvage and J.F. Petroff, in /1/, Vol. 1b.

/38/ T. Hosokawa et al., Rev. Sci. Instr. 60 (7) (1989) 1779.

/39/ N. Takahashi et al., Proc. SPIE 923, (1988) 47.

/40/ J.P. Silverman et al., J. Vac. Sci. Technol. B11 (1993) 2976.

/41/ M.N. Wilson et al., Microelectronics Eng. 11 (1990) 225.

/42/ W.A. Johnson (Motorola), X-ray Lithography - Status and Projected Use, Proc. IEEE Particle Accelerator Conference May 1-5 1995, Dallas 1995.

/43/ W.D. Grobman, in /1/ Vol 1b.

/44/ R. Dammel, SPIE PRess, Vol 11, Bellingha, WA (1993).

/45/ C.J. Progler et al., J. Vac. Sci. Technol. B11 (1993) 2888.

/46/ R. Viswanathan et al., J. Vac. Sci. Technol. B11 (1994) 2910.

/47/ K. Deguchi, J. Photopolymer Sci. Technol. 6 (1993) 445.

/48/ J.R. Maldonado, SPIE Proc. vol 1465, (1991) 2.

/49/ M. Oda and H. Yoshihara, Mat. Res. Soc. Symp. Proc., 306 (1993) 69.

/50/ E.W. Becker et al., Microelectron. Eng., 4 (1986) 35-56.

/51/ A. Michel et al., Abformiung von Mikrostrukturen auf prozessierten Wafern, Internal Report 5171, Kernforschungszentrum Karlsruhe, 1993.

/52/ C. Burbaum et al., Sensors Mater. 3 (2) (1991) 75-85.

/53/ M. Harmening et al., Proc. Micro Electro Mechanical Systems 1992, IEEE Cat. No. 0-7803-0497-7/92 (1992) 202-207.

/54/ P. Bley, Inter. Sci. Rev. 18 (1993) 267-272.

/55/ C. Müller and J. Mohr, Inter. Sci. Rev. 18 (1993) 273-279.

/56/ ELETTRA Conceptual Design Report, Sincrotrone Trieste, 1989.

/57/ Marks, N., Barnes, P., Synchrotron Radiation News, Vol. 6, No. 6, (1993), 7.

/58/ I. Arcon and S. Bernstorff, Multipurpose High Resolution X-Ray Beam Line At ELETTRA - The Conceptual Design, this report chapter III.

/59/ P. Engström et al., Nucl. Instr. Meth. B26 (1989) 222.

/60/ P. Engström et al., Nucl. Instr. Meth. in Phys. Res. A302 (1991) 547.

/61/ B.P. Tonner, Ultramicroscopy 36 (1991) 130.

/62/ D. Abramič et al. (The BOSS Collaboration), A Multipurpose X-ray Beamline at ELETTRA, Jožef Stefan Institute Internal Report, DP-7083, October 1994.

Dr. Mark Pleško, dipl.ing.
Institut "Jožef Stefan"
Jamova 39, POB 100, 61111 Ljubljana,
Tel.: +386 61 1773 900
Fax: +386 61 1261 029
E-mail: Mark.Plesko @ijs.si

Prispelo (Arrived): 28.09.1995 *Sprejeto (Accepted): 07.11.1995*